Two-photon spectroscopy: A technique for characterizing diode-laser noise

Robert E. Ryan
Department of Physics, State University of New York, Stony Brook, New York 11794

Lynn A. Westling
Department of Physics, Swarthmore College, Swarthmore, Pennsylvania 19081

Reinhold Blümel
Laboratory for Plasma Research, University of Maryland, College Park, Maryland 20742

Harold J. Metcalf
Department of Physics, State University of New York, Stony Brook, New York 11794
(Received 14 December 1994)

Using Doppler-free Rb two-photon excitation measurements, we present support for the hypothesis that semiconductor-laser noise is characterized by pure phase-diffusion noise. We measured near-Lorentzian shapes for both the laser and the two-photon excitation spectra and a slope of 3.7 ± 0.3 for the dependence of the two-photon excitation width on the laser width. These represent measurements of the second-order field statistics of a naturally operating laser where the noise is dominated by spontaneous emission. The measured spectral shape and slope are in excellent agreement with the Mollow model, which predicts a Lorentzian spectral shape and a slope of 4 for weak-field, two-photon excitation with a pure phase-diffusion field (Lorentzian spectral density). The dominance of phase-diffusion noise is further corroborated by an analytically solvable microscopic noise model that includes phase and amplitude noise.

PACS number(s): 42.55.Px, 32.80.−t, 32.70.Jz, 42.50.Lc

I. INTRODUCTION

Most modern experiments in quantum and nonlinear optics use lasers as light sources. Thus it is desirable to understand the effects of laser noise on these phenomena since such effects depend strongly on the statistical properties of the radiation field [1,2]. In this paper we invert this point of view and exploit a nonlinear optical effect as a tool for characterizing the stochastic processes inherent in a particular laser source [3].

A simple but fairly realistic noise model for a stable, single-mode cw laser operating well above threshold maintains that the amplitude of the laser field is constant and that the optical phase exhibits a random walk caused by spontaneous emission. The motivation for this model is based on the following observations. Above threshold, the field amplitude is stabilized by gain saturation and is thus relatively constant about some operating value [1]. The phase of the laser field, however, has no natural stabilizing mechanism. Such noise is referred to as phase-diffusion noise, and its phasor diagram is shown in Fig. 1. Since the magnitude of the field fluctuates very little and the phase can change by any value, the phasor diagram is approximately a circle. Also shown in Fig. 1 is the phasor diagram of a chaotic field, which might result from the output of a lamp, a multimode laser, or a single-mode laser emitting light below threshold. Since a chaotic field does not possess any intensity stabilization mechanism, the field can take on any value in a two-dimensional region of the complex plane centered about the origin [4].

It is important to note that these two types of fields can have the same spectral density and thus the same first-order correlation function. The fundamental differences in the statistics of these fields are manifest only in the higher-order correlation functions. The term "higher order," here and throughout this paper, refers to all orders larger than the first. A linear system will not be able to distinguish between fields with the same spectral density even if the higher-order correlation functions differ. Differences in the observables occur only in the excitation of nonlinear systems. This requirement motivates the use of a nonlinear optical transition for the characterization of laser noise.

Two-photon excitation provides the simplest tool for

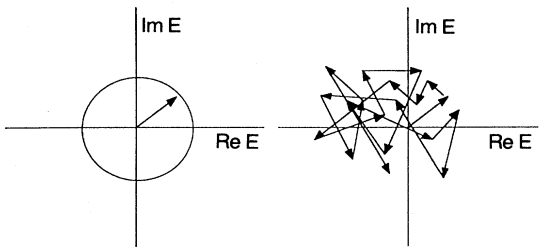

FIG. 1. Phasor diagram of a phase-diffusion field (left) and a chaotic field (right).

observing the effects of the second-order statistical properties of light. The simplicity arises because the weak-field two-photon excitation can be approximately described by second-order perturbation theory involving only the second-order field correlation function [5]. In addition, two-photon spectroscopy, implemented in its Doppler-free form, is a powerful technique because it allows the study of atoms and molecules in a simple cell in the gas phase without the need of atomic beams for the reduction of Doppler broadening. It is important to eliminate the Doppler broadening to avoid masking the statistical properties of the optical field.

The theory for weak-field two-photon excitation by a fluctuating field was developed by Mollow [5]. For a stationary field with Gaussian statistics, he showed that the weak-field two-photon absorption spectrum is the Fourier transform of the second-order correlation function of the electric field. Furthermore, he calculated the two-photon excitation rates with both phase-diffusion and chaotic fields that have a Lorentzian spectral density and found that in both cases the two-photon transition width is directly proportional to the laser width. The proportionality factor (slope), however, depends crucially on the statistical nature of the exciting laser field: It is 4 for a phase-diffusion field and 2 for a chaotic field (see Fig. 2). (A slope of unity is expected for a linear process.) Higher-order correlation functions can be studied with higher-order photon processes [6].

A short note on our usage of "absorption signal" and "fluorescence signal" in this paper is in order now. It is well known that the photon statistics of the exciting light beam and the photon statistics of the fluorescence signal can be vastly different (see, e.g., [7]). Therefore, in general, there is a problem in inferring statistical properties of the absorbed light from the statistical properties of the fluorescence light. In the work reported in this paper, however, we infer statistical properties indirectly from the respective widths of the incident light and the fluorescence signal which involves time averages over a vast number of absorption and emission events. Therefore, for the purposes of this paper, we are only concerned with the macroscopic energy fluxes of absorbed and emitted light. Consequently, within the framework of our experiments reported here, we are justified in using the working hypothesis "absorption signal = luminescence signal."

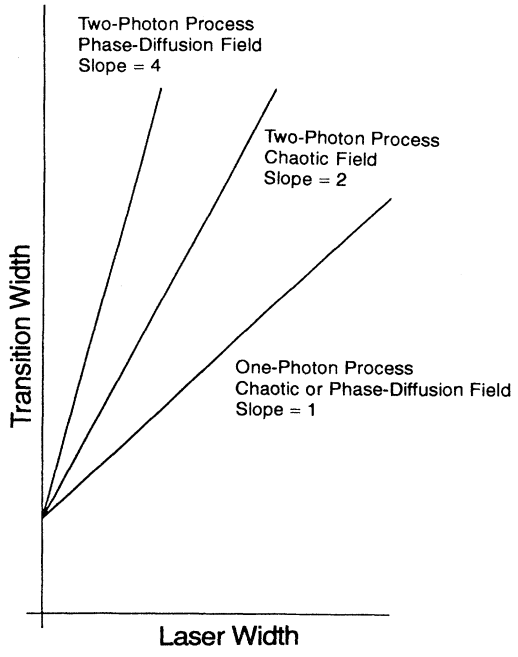

FIG. 2. Predicted behavior of the transition widths for Lorentzian excitation spectral densities for both chaotic and phase-diffusion fields for one- and two-photon processes.

In order to test some of the stochastic excitation models, several groups have used sources of technically generated laser noise with known statistical properties to drive nonlinear atomic transitions [8,9]. These sources included controlled phase, frequency, and amplitude noise of several varieties. At the Joint Institute for Laboratory Astrophysics (JILA), a host of phenomena ranging from saturated fluorescence to two-photon spectroscopy has been studied with such an artificially broadened laser source consisting of a highly stabilized cw dye laser whose light was modulated externally by filtered noise sources of known statistics. The electronic filters and the modulation amplitude were adjusted so that the resulting laser field simulated a phase-diffusion field [8]. The most extensive two-photon absorption experiments were conducted using the Na $3S$-$5S$ transition with this source [10]. These experiments showed that Lorentzian phase-diffusion fields produce a slope of 4 as a function of the laser width for two-photon transitions, in agreement with the Mollow theory [10]. In addition, two-photon transitions excited with Gaussian spectral density phase-diffusion fields were investigated both experimentally and theoretically [11]. Unlike the Lorentzian case, phase-diffusing Gaussian spectral densities produced Gaussian two-photon spectral shapes with a slope of 2.

Although the investigations reported in Refs. [10] and [11] were conducted using technical noise which is not necessarily characteristic of naturally operating lasers, indications for the relevance of some of the subtleties reported in Refs. [10] and [11] can be found in the literature. For example, experiments were reported where cw dye lasers were used to drive two-photon transitions in Na ($3S$-$5S$) and Rb ($5S$-mS, $5S$-mD) [12]. The resulting width of the two-photon transition turned out to be approximately twice the laser width [12]. No explanation was offered for this observation other than attributing the enhanced line-broadening effects to laser jitter. However, for many lasers such as dye lasers that are technically phase-noise limited, Gaussian spectral densities arise [13]. Therefore we point out here that the broadening measured in Ref. [12] is consistent with the results reported in Refs. [10] and [11] assuming that the technical noise of the lasers used in Ref. [12] had the expected Gaussian spectral density.

In this paper we report our study of the noise properties of semiconductor lasers, chosen because they are

becoming ever more important in laser spectroscopy and atomic and molecular physics. We use nonlinear optical processes for the characterization of laser noise, and we employ atoms as detectors for the second-order field correlation function. We do this by studying the effects of semiconductor diode laser noise in Doppler-free two-photon spectroscopy in Rb. The experimental investigation reported here uses Mollow's predictions to study the statistics of a naturally operating laser.

Semiconductor lasers are also one of the few types whose noise properties approximate a phase-diffusion field, with fundamental limits imposed by quantum mechanics and not by technical noise. The dominance of the fundamental quantum noise in semiconductor lasers makes them useful for the study of fundamental stochastic excitation. In addition, they serve as a unique light source for the experimental verification of the quantum theory of lasers. Diode lasers, for example, provide a major testing ground for the modified Schawlow-Townes formula [13]. In practice, however, the sensitivity of semiconductor lasers to optical feedback can cause severe problems. These effects are covered in detail in a previous paper [14].

Doppler-free two-photon spectroscopy is a valuable tool for studying narrow resonances. It has been used by atomic spectroscopists to measure hyperfine structure, isotope shifts, Stark shifts, Zeeman splittings, Lamb shifts, and the Rydberg constant of many different atoms and molecules [15]. Two-photon transitions can be quite narrow; Rydberg states can be excited by two-photon transitions of width 1 kHz or less [16]. Many other transitions have widths of tens of kHz. A two-photon transition of fundamental importance is the $1S$-$2S$ transition in hydrogen that has a natural width of ~ 1 Hz, making it suitable for use in atomic clocks and frequency standards of unprecedented accuracy and precision. To study these narrow transitions requires extremely narrow lasers so that the effects of finite laser bandwidth need not be considered. At present, however, most tunable lasers are wider than such narrow transitions and the finite bandwidth of the laser must be taken into account.

II. CHARACTERISTICS OF SEMICONDUCTOR-LASER NOISE

In this section we review some of the noise characteristics of single-mode continuous wave (cw) semiconductor lasers. We emphasize phase-diffusion noise caused by spontaneous emission, since this was demonstrated to be the dominant noise mechanism in semiconductor lasers [17–22]. It is also a fundamental source of noise in other cw lasers [23,24]. Other fundamental noise sources such as amplitude fluctuation due to partition noise [25] are relatively small above threshold [17,18]. Although intensity noise can be important in some atom-field interactions, the stabilizing feature of gain saturation minimizes the effects in cw lasers to typically less than 1%.

In order to assure that the noise effects we observe are caused only by spontaneous emission in the semiconductor medium, we must first ensure that all other sources of technical noise are under control. One important source of technical noise is current fluctuations in the power supply of the laser. Diode lasers are one of the few types of lasers that show an increased linewidth directly related to pump noise [26]. Current fluctuations, arising from Johnson noise, shot noise, or electromagnetic noise pick-up, can produce fluctuations in the laser frequency, power, and linewidth. Using current to tune $Al_xGa_{1-x}As$ lasers by less than 1 MHz results in a tuning coefficient of approximately -3 GHz/mA. For shifts larger than 1 MHz, the tuning coefficient is on the order of -300 MHz/mA. It increases near the relaxation oscillation to 1 GHz/mA [27]. Thus, for a laser operating far above threshold with a linewidth of approximately 10 MHz, the rms current noise should not exceed 300 nA if its contribution to the laser's spectral width is to be smaller than 10%. This condition is easily fulfilled with a simple battery power supply.

A less fundamental but no less important effect on the noise is the influence of optical feedback on diode lasers. Since optical feedback can dominate both the static and dynamic properties of the diode's output (even with 60 dB or more of optical isolation [14]), we invested a great deal of effort (see Sec. IV) to minimize its effects [14,28,29]. Our results indicate that, even in the presence of a small amount of residual optical feedback, phase-diffusion noise dominates.

At present, semiconductor lasers are the only lasers that require a quantum-mechanical description of their noise characteristics for all regions above threshold. Quantum effects are not important for the noise properties of most other lasers operated well above threshold as the quantum effects are masked by extrinsic or technical noise. Figure 3 compares the behavior of predominantly technical and quantum-limited lasers. The fundamental linewidth of most cw lasers is inversely proportional to the laser power. This is indicated in Fig. 3 as the solid lines sloping upward. The horizontal line in Fig. 3 illustrates a power-independent technical noise source that dominates when the quantum-limited laser noise is less

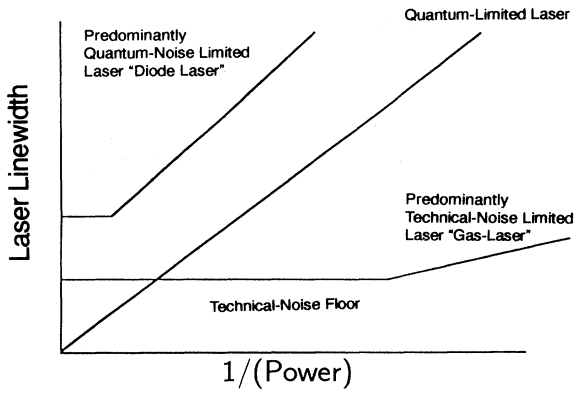

FIG. 3. Behavior of linewidth as a function of inverse laser power for quantum-limited lasers, predominantly quantum-limited (diode) lasers, and predominantly technical-noise-limited (gas) lasers.

than the technically induced linewidth. For example, although a standard He-Ne laser has a measured linewidth greater than tens of kHz, its fundamental linewidth would be less than 1 Hz. In contrast, the fundamental noise in semiconductor lasers is generally several orders of magnitude larger than its solid-state or gas-laser counterparts, and is typically larger than the technical noise. In this case, the laser noise is quantum limited over a wide range of power. The large linewidth derives from the small cavity length of semiconductor lasers (only a few hundred micrometers), and low-reflectivity mirrors, each of which contributes to low energy storage in the laser cavity. Also, there is a linewidth enhancement factor α to be explained below.

Because of their large fundamental linewidth, semiconductor lasers are ideal light sources for the investigation of quantum noise. The first systematic measurements of the linewidth and line shape of semiconductor lasers were conducted by Fleming and Mooradian with a Fabry-Pérot interferometer [19]. They showed that the spectral shapes of $Al_xGa_{1-x}As$ semiconductor lasers were predominantly Lorentzian and that the linewidth decreased in inverse proportion to the laser power. Their measurements showed that the linewidths were 30 times greater than expected on the basis of the modified Schawlow-Townes formula. Henry parametrized the Fleming and Mooradian results by introducing the linewidth enhancement factor α that increases the linewidth by a factor $(1+\alpha^2)$. This factor is defined as [18]

$$\alpha=2\frac{\omega_0\Delta\mu}{c\Delta g}\ , \tag{2.1}$$

where ω_0 is the angular frequency of the laser mode, c is the speed of light, $\Delta\mu$ is the change in index of refraction, and Δg is the change in gain. Besides the enhancement factor α that describes a coupling of amplitude and phase noise, incomplete population inversion from Fermi-Dirac statistics at finite temperature is important [17,18].

Gain changes caused by spontaneous emission also result in a variation of the index of refraction and result in additional phase fluctuations. These additional fluctuations result from intensity relaxation oscillations that manifest themselves as small sidelobes or satellites in the laser frequency spectrum. The amplitudes of sidelobes are typically 1% or less compared with the main Lorentzian [30,31]. Vahala, Harder, and Yariv have measured an asymmetry in these satellites of about 20%. This result can be deduced if intensity fluctuations are included in the analysis of the line shape [31].

At very high power, the semiconductor-laser linewidth is not necessarily inversely proportional to power but can be independent of power over some range. Welford and Mooradian saw power-independent line broadening in $Al_xGa_{1-x}As$ diode lasers, especially at lower temperatures [21]. The origin of the linewidth floor is not well understood, and several theories have been suggested: carrier-density fluctuations, light scattering, current noise, $1/f$ noise, spatial and spectral hole burning [32–35]. However, over the power ranges employed in our experiments using the Sharp LT021 semiconductor laser, we did not observe any evidence for this effect.

III. THEORY

Unlike linear spectroscopy, where the width of an atomic transition is determined by the convolution of the laser and atomic spectral shapes, the width and shape of a multiphoton transition are not simply related to the laser and the natural atomic line shape. Thus nonlinear spectroscopy is a sensitive measure of the higher-order statistics of light. In this section we discuss several simple and analytically solvable noise models that provide the basis for the discussion of the experimental results presented in Sec. IV. In Sec. III A we briefly review Mollow's theory for the one- and two-photon absorption widths. For the sake of completeness this theory is then applied to chaotic light fields (Sec. III A), light fields with pure frequency noise (Sec. III B), and light fields with pure phase noise (Sec. III C). The main focus will be on Sec. III D where we present a microscopic noise model that incorporates both amplitude and phase noise, and allows for various degrees of correlation between them. The results of this model provide our principal argument for attributing the observed slope in our experiments to the prevalence of phase noise in the exciting semiconductor-laser light.

A. Brief review of Mollow's theory

Consider a weak-field one-photon process where first-order perturbation theory holds (linear process) with a natural full width at half maximum (FWHM) of κ_f, where the excitation field has a Lorentzian spectral density with a FWHM of $2b$. Then, the one-photon transition rate W_1 is proportional to a Lorentzian according to

$$W_1\sim I\frac{b+\kappa_f/2}{(b+\kappa_f/2)^2+(\omega_0-\omega_f)^2}\ , \tag{3.1}$$

where I is the intensity of the exciting light field. Moreover, for $\kappa_f \ll 2b$, the FWHM of W_1 is $2b$ which is the same as the linewidth of the exciting light. Therefore the slope in this case is 1. This result is illustrated in Fig. 2.

The two-photon theory presented in this section rests on the work of Mollow [5]. For weak fields where second-order perturbation theory holds, he showed that the two-photon transition rate $W_2(\omega)$ is the Fourier transform of the second-order field correlation function

$$G^{(2)}_{\omega}(t)=\langle E^*(-t)E^*(-t)E(t)E(t)\rangle$$

according to

$$W_2(\omega)\sim\int_{-\infty}^{\infty}G^{(2)}_{\omega}(t)\exp(2i\omega_f t-\kappa_f|t|)dt\ , \tag{3.2}$$

where ω is the frequency of the light exciting the two-photon transition, ω_f is the resonance frequency of the transition, and κ_f is its natural width. The spectral distribution function $S(\omega)$ of the exciting light field $E(t)$ with carrier frequency ω_0 is related to the first-order field correlation function $G^{(1)}_{\omega_0}(t)=\langle E^*(0)E(t)\rangle$ (first-order

temporal coherence) according to [36]

$$S(\omega)\sim\int_{-\infty}^{\infty}G^{(1)}_{\omega_0}(t)\exp(i\omega t)dt\ . \tag{3.3}$$

For a chaotic light source, the correlation functions $G^{(1)}_{\omega_0}$ and $G^{(2)}_{\omega}$ are worked out explicitly in Ref. [36]. The result is

$$\begin{aligned}&G^{(1)}_{\omega_0}(t)\sim\exp(-i\omega_0 t-\Gamma|t|)\ ,\\&G^{(2)}_{\omega}(-t,-t;t,t)\sim\exp(-4i\omega t-4\Gamma|t|)\ ,\end{aligned} \tag{3.4}$$

where Γ is the damping constant that summarizes the effects of all linewidth-broadening mechanisms such as radiative and collisional broadening. Using (3.4) in (3.3) and (3.2) yields

$$S(\omega)\sim 2\Gamma/[(\omega-\omega_0)^2+\Gamma^2] \tag{3.5}$$

and

$$W_2(\omega)\sim(\kappa_f/2+2\Gamma)/[(\omega_f-2\omega)^2+(\kappa_f/2+2\Gamma)^2]\ , \tag{3.6}$$

respectively. For $\kappa_f\ll\Gamma$, $W_2(\omega)$ is a Lorentzian with width 2Γ, whereas $S(\omega)$ is a Lorentzian with width Γ. Therefore, for chaotic light, the linewidth of the two-photon signal is twice the bandwidth of the exciting light and the slope is 2. This result is also illustrated in Fig. 2.

B. Two-photon line shapes for pure frequency noise

In the case of pure frequency noise well modeled by a Gaussian random process, the line shape of the exciting light as well as the two-photon signal are both Gaussian. This is easily demonstrated in the following way. Suppose that g is a Gaussian random variable with $\langle g\rangle=0$ and $\langle g^2\rangle=1$, and Ω is the amplitude of the frequency noise of a light field with carrier frequency ω_0 according to $E(t)=\exp(-i[\omega_0+\Omega g]t)$. The first-order field correlation function for this type of light field is given by

$$G^{(1)}_{\omega_0}(t)=\exp(-i\omega_0 t)\exp(-\Omega^2t^2/2) \tag{3.7}$$

and the second-order field correlation function is

$$G^{(2)}_{\omega_0}(t)=\exp(-4i\omega_0 t)\exp(-8\Omega^2t^2)\ . \tag{3.8}$$

The spectral distribution function is

$$S\sim\exp[-(\omega-\omega_0)^2/2\Omega^2] \tag{3.9}$$

and the two-photon transition rate is

$$W_2\sim\exp[-(\omega_f-2\omega)^2/8\Omega^2]\ . \tag{3.10}$$

Both have a Gaussian shape. The width of W_2 is twice the width of S. This means that the slope in this case is 2.

C. Two-photon line shapes for pure phase noise

So far we have discussed two examples of noise processes that lead to a slope of 2 in two-photon excitation experiments. Next, we discuss pure phase noise that results in a slope of 4. The different slopes are a signature of the underlying noise processes and thus provide a spectroscopic tool for identifying the statistical nature of the noise.

Consider the following noise process where the phase ϕ changes randomly at equidistant time intervals Δt according to

$$\phi_{j+1}=\phi_j+\sigma g_j\ , \tag{3.11}$$

where g_j is a Gaussian random variable with

$$\langle g_j\rangle=0\ \text{ and }\ \langle g_jg_k\rangle=\delta_{jk}\ . \tag{3.12}$$

The recurrence equation (3.11) can be solved explicitly:

$$\phi_j=\phi_0+\sigma\sum_{k=0}^{j-1}g_k\ . \tag{3.13}$$

With (3.12) and (3.13) it can be shown that the phase undergoes a diffusion process according to

$$\langle\phi_j\rangle=0,\quad\langle\phi_j^2\rangle=\phi_0^2+Dt,\quad D=\sigma^2/\Delta t\ . \tag{3.14}$$

A model for a phase-diffusing light field is given by

$$E_j=\bar{E}\exp[-i(\omega_0t+\phi_j)]\ , \tag{3.15}$$

where $\bar{E}$ is a constant field amplitude. The first-order field correlation function for this model is given by

$$\begin{aligned}G^{(1)}(t_k)&=\langle E^*(t_0)E(t_k)\rangle\\&=\bar{E}^{\,2}\exp(-i\omega t_k)\langle\exp[-i(\phi_k-\phi_0)]\rangle\\&=\bar{E}^{\,2}\exp(-i\omega_0t_k-Dt_k/2)\ .\end{aligned} \tag{3.16}$$

In this expression we used (3.12), (3.13), and the identity $\langle\exp(\beta g)\rangle=\exp(-\beta^2/2)$, which holds for arbitrary real β. Since (3.16) does not depend on the time step Δt it can be generalized to

$$G^{(1)}(t)=\bar{E}^{\,2}\exp[-i\omega_0t-D|t|/2]\ .$$

With this result the spectral distribution function S is given by

$$S(\omega)=\bar{E}^{\,2}D/[(\omega-\omega_0)^2+(D/2)^2]\ . \tag{3.17}$$

In the same way the second-order field correlation function $G^{(2)}_{\omega}$ is calculated and yields the result

$$G^{(2)}_{\omega}(t)=\bar{E}^{\,4}\exp(-4i\omega t)\exp(-4D|t|)\ . \tag{3.18}$$

Therefore, the two-photon transition rate is

$$W_2(\omega)\sim(4D+\kappa_f)/[(\omega_f-2\omega)^2+(2D+\kappa_f/2)^2]\ . \tag{3.19}$$

Both (3.17) and (3.19) are Lorentzians with widths $D/2$ and $2D$, respectively, if $\kappa_f\ll D$. Thus the slope for a two-photon transition with a pure phase-diffusion field is 4 (see Fig. 2).

D. Two-photon line shapes for combined amplitude and phase noise

Finally, we introduce here a noise model which is closer to the physics of a semiconductor laser and includes phase noise, amplitude noise, and relaxation

effects. The light field of the semiconductor laser is modeled by a stochastic process resembling the pure phase-noise field discussed above and given by

$$\begin{aligned} E_j &= E_j \exp[i(\omega_0+\phi_j)] , \\ E_{j+1} &= E_j+\epsilon_1 g_j^{(1)}+\epsilon_2 g_j^{(2)}-K(E_j-\bar{E}) , \\ \phi_{j+1} &= \phi_j+\sigma g_j^{(2)} . \end{aligned} \tag{3.20}$$

Here, $g_j^{(1)}$ and $g_j^{(2)}$ are Gaussian random variables with $\langle g_j^{(r)}\rangle=0$ and $\langle g_j^{(r)} g_k^{(s)}\rangle=\delta_{jk}\delta_{rs}$, respectively, and $K(E_j-\bar{E})$ is gain clamping to be discussed below. The noise term proportional to ϵ_2 in (3.20) describes amplitude noise which is correlated with the phase noise [$g_j^{(2)}$ also appears in the ϕ equation in (3.20)] whereas the noise term proportional to ϵ_1 describes uncorrelated amplitude noise [$g_j^{(1)}$ does not appear in the ϕ equation in (3.20)]. Using the techniques outlined in Sec. III C above and $D_{1,2}=\epsilon_{1,2}^2/\Delta t$, we derive the spectral density S and the two-photon transition rate W_2 for the field (3.20) and obtain

$$S(\omega)\sim\frac{D_1+D_2}{2K\bar{E}^2[(\omega-\omega_0)^2+(K+D/2)^2]}+\frac{D/2}{(\omega-\omega_0)^2+(D/2)^2}-\frac{(\omega-\omega_0)(D+K)(DD_2)^{1/2}}{\bar{E}[(K+D/2)^2+(\omega-\omega_0)^2][(D/2)^2+(\omega-\omega_0)^2]} , \tag{3.21}$$

and

$$\begin{aligned} W_2(\omega)\sim\mathrm{Re}\Bigg\{ & A\frac{2D+\kappa_f/2+2K+i(\omega_f-2\omega)}{(2D+\kappa_f/2+2K)^2+(\omega_f-2\omega)^2} \\ & +B\frac{2D+\kappa_f/2+K+i(\omega_f-2\omega)}{(2D+\kappa_f/2+K)^2+(\omega_f-2\omega)^2} \\ & +C\frac{2D+\kappa_f/2+i(\omega_f-2\omega)}{(2D+\kappa_f/2)^2+(\omega_f-2\omega)^2}\Bigg\} , \end{aligned} \tag{3.22}$$

where

$$\begin{aligned} A &= G_0-B-C , \\ G_0 &= \bar{E}^4+3(D_1+D_2)\left[4\bar{E}^2+\frac{(D_1+D_2)}{K}\right] , \\ B &= 4\left[\bar{E}+2i\frac{(DD_2)^{1/2}}{K}\right] \\ &\quad\times\left[\frac{\bar{E}(D_1+D_2)}{2K}-i\frac{F_0(DD_2)^{1/2}}{K}\right] , \\ F_0 &= \bar{E}^2+\frac{(D_1+D_2)}{2K} , \\ C &= \frac{F_0}{2K}\left\{2K\left[\bar{E}+2i\frac{(DD_2)^{1/2}}{K}\right]^2+(D_1+D_2)\right\} . \end{aligned} \tag{3.23}$$

It turns out that the shape of the laser's spectral density S as well as the shape of the two-photon signal W_2 are more complicated than just a single Lorentzian. Therefore, the widths of S and W_2 are not known without a more detailed knowledge of the magnitudes of the parameters in (3.21) and (3.22). Therefore we will now estimate these parameters for an $Al_xGa_{1-x}As$ diode laser.

The constant K in (3.20) describes the relaxation of the semiconductor-laser field back to its average value $\bar{E}$ after a spontaneous emission event. According to Ref. [17] this relaxation occurs on a time scale of 1 ns, which implies $K\sim10^9\ \mathrm{s}^{-1}$.

Next, we determine the phase-diffusion constant D. According to (3.14), $\langle\phi^2\rangle\sim Dt$ which can be equated to Henry's expression for the phase-diffusion constant [17] and yields

$$D=R(1+\alpha^2)/2I . \tag{3.24}$$

Here, R is the spontaneous emission rate for the semiconductor laser ($R\approx8\times10^{11}\ \mathrm{s}^{-1}$), I is the laser intensity (normalized such that it also equals the number of photons in the laser cavity [17,37]), and α is the linewidth enhancement factor which was taken to be 5 [17].

The diffusion constant D_2 that describes the correlated amplitude and phase noise can also be related to Henry's model. There, the amplitude-noise process is given by $E_{j+1}=E_j+\cos(\theta_j)$, where $E_j=(I_j)^{1/2}$ is the electric-field amplitude of the laser at the time the jth emission takes place and θ_j is the phase angle of the spontaneous emission photon. The phase-noise process is (neglecting the constant term)

$$\begin{aligned} \phi_{j+1} &= \phi_j+[\sin(\theta_j)-\alpha\cos(\theta_j)]/\bar{E} \\ &= \phi_j+(1+\alpha^2)^{1/2}\sin[\theta_j+\psi(\alpha)]/\bar{E} , \end{aligned} \tag{3.25}$$

where $\psi(\alpha)$ is a constant phase angle that depends only on α. In our model we take $\sin[\theta_j+\psi(\alpha)]$ to be a Gaussian random variable. This may seem like a crude approximation, but for the case of many spontaneous emissions and because of the central-limit theorem, both models become equivalent. In order to determine ϵ_2 we demand

$$\begin{aligned} &\langle\epsilon_2 g^{(2)}\exp[i\sigma g^{(2)}]\rangle \\ &\quad=\langle\cos(\theta)\exp\{i[\sin(\theta)-\alpha\cos(\theta)]/\bar{E}\}\rangle . \end{aligned} \tag{3.26}$$

The parameter σ in (3.26) can be calculated using (3.14), (3.24), and $\Delta t = 1/R$. We obtain

$$\sigma = \{(1+\alpha^2)/2I\}^{1/2} . \tag{3.27}$$

Since $\sigma \ll 1$, the exponent on the left-hand side of (3.26) can be expanded to first order in σ. Using $\langle g^{(2)} \rangle = 0$ and $\langle g^{(2)} g^{(2)} \rangle = 1$, we obtain

$$\langle \epsilon_2 g^{(2)} \exp(i\sigma g^{(2)}) \rangle \approx i\epsilon_2 \sigma . \tag{3.28}$$

Likewise, since $|\bar{E}| = I^{1/2} \gg 1$ the right-hand side of (3.26) can be expanded to first order in $1/\bar{E}$ and yields

$$\langle \cos(\theta) \exp\{i[\sin(\theta) - \alpha\cos(\theta)]/\bar{E}\} \rangle \approx -i\alpha/2\bar{E} . \tag{3.29}$$

We used $\langle \cos(\theta)\sin(\theta) \rangle = 0$ and $\langle \cos(\theta)^2 \rangle = \frac{1}{2}$. Equating (3.28) and (3.29) we can solve for ϵ_2. Using the result (3.27) for σ and $\bar{E}^2 = I$ we obtain

$$D_2 = \epsilon_2^2/\Delta t = R\alpha^2/2(1+\alpha^2) . \tag{3.30}$$

Inspection of the result for W_1 shows that it is advantageous to define

$$d_2 = D_2/I = R\alpha^2/2I(1+\alpha^2) . \tag{3.31}$$

This allows direct comparison between D and d_2 and shows that $d_2 \sim D/\alpha^2$.

Close to the center of the laser line the third term in (3.21) does not contribute, and the width of the line is determined by the first two terms. The width of the laser line measured in our experiments (see Sec. IV) is on the order of 15 MHz. Since the width of the first term in (3.21) is on the order of 1 GHz, the width of the laser line is clearly determined by the phase-diffusion constant D in the second term.

The two-photon line shape can be discussed in similar ways. In this case the third term in (3.22) is dominant. For $\kappa_f \ll D$, the width of the third term in (3.22) is four times the width of the second term in (3.21) and thus the slope predicted by the model defined in (3.20) is 4. Since this model incorporates the major elements of semiconductor noise, a slope of 4 is the expected result for the two-photon experiments on Rb which will be described in the following section. Thus the theoretical model supports our intuition that phase-diffusion noise dominates in our experiments.

IV. EXPERIMENT

In this section we describe our experiments for measuring two-photon excitation spectra of Rb using diode-laser light. The experimental setup is presented in Sec. IV A. The two-photon measurements are described in Sec. IV B. Use of temperature tuning to obtain quantum-limited stochastic excitation is described in Sec. IV C and our measurements directly addressing the nature of the diode-laser noise are reported in Sec. IV D.

A. Description of the setup

A block diagram of the experimental setup is shown in Fig. 4. The light from a 10-mW Sharp LT021 MD diode

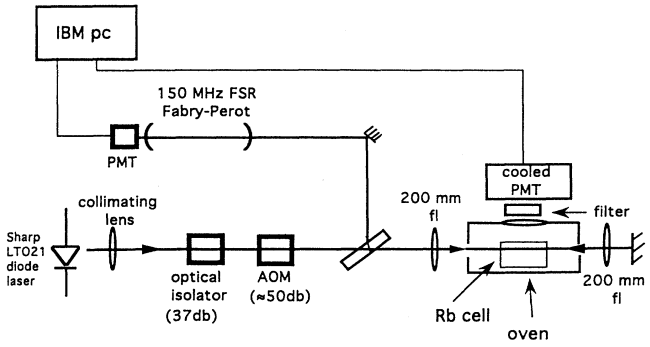

FIG. 4. Two-photon spectroscopy apparatus.

laser is focused into and then retroreflected back through a Rb cell. The laser was operated in a dry-air-purged plastic cylindrical container that kept the laser from frosting when cooled, minimized ambient temperature fluctuations, and reduced acoustic vibrations. Purging was chosen over a desiccant so that a window would not be needed, since windows can be a source of feedback. The laser was tuned to 778.1 nm (twice the $5S_{1/2}$-$5D_{5/2}$ Rb vacuum wavelength) by both temperature and current tuning.

The temperature was controlled to better than 0.5 mK by a circuit consisting of a thermistor in a Wheatstone bridge and an analog proportional controller to adjust the current of a Peltier cooler in thermal contact with the laser. Flowing tap water through the copper heat sink of the Peltier cooler minimizes long-term drifts in the temperature controller. (The temperature of the tap water used does not fluctuate by more than 1 °C over the time span of a year.)

Battery supplies were chosen to minimize noise from current fluctuations. A 6-V, 20-A h gel cell battery powered the laser through a resistive network. A 10-Ω resistor in series with the laser was used to monitor the laser current with a Fluke 77 multimeter. Current tuning was performed with a filtered Hewlett Packard 3415 function generator. The current filtering was a single pole RC network placed across the current-measuring resistor and diode laser in the laser power supply.

The Rb oven shown in Fig. 4 consisted of an insulated aluminum box painted black to reduce stray scattered light. The oven was heated with four soldering irons, whose temperature was controlled by a Variac, to typically 125 °C. The oven contained a Rb Opthos Instruments cell 100 mm long and 25 mm in diameter equipped with optical-quality windows to minimize scattering and aberration of the beam. The irons were placed to heat preferentially the cell windows in order to prevent rubidium from condensing on them. The cell was supported by a black anodized aluminum structure and a black-painted aluminum tube that acted as both support and baffling. The baffling was designed to hide the detector from the oven heaters, thereby reducing the background from the heating elements by at least three orders of magnitude. The temperature was measured with a K-type thermo-

couple placed near the coldest part of the cell.

Since our main goal is to study the laser noise using two-photon spectroscopy, we have chosen to use a Fabry-Pérot interferometer as both a frequency marker and laser characterization system [38]. High-quality Fabry-Pérot interferometers operating close to the theoretical performance limit also allow relatively easy deconvolution of the instrumental response from the measured spectral shapes, as long as the laser spectral shapes are Lorentzian or Voigt profiles. This ease of deconvolution arises from (1) the nearly Lorentzian instrumental shape of a single transmission peak of high-quality interferometers, and (2) the fact that the convolution of two Lorentzians is another Lorentzian with a width equal to the sum of the widths of the input Lorentzians. Fabry-Pérot interferometers, however, can introduce artifacts because of insufficient resolution and free spectral range. To overcome these difficulties, we found that it is essential to know the instrumental response and, wherever possible, use Fabry-Pérot interferometers of appropriate free spectral ranges and resolution.

Although high-resolution Fabry-Pérot interferometers are superb instruments for determining the spectral shape and width of diode lasers, they are extremely sensitive to mirror spacing and alignment. A convenient way to get a scanning confocal Fabry-Pérot interferometer (CFPI) operating near its theoretical performance limit is to use a light source significantly narrower than the instrumental response of the CFPI and to adjust the mirror spacing and alignment while observing the response. However, at typical $Al_xGa_{1-x}As$ semiconductor-laser wavelengths operating around 800 nm, few readily available inexpensive narrow-band laser sources exist. The wavelengths of HeNe- and argon-laser lines are too different to be of any use, since very-high-reflectance coatings used for the Fabry-Pérot interferometer mirrors typically have spectral width less than 100 nm. Even if a narrow laser source is available, such as an external cavity laser or dye laser, it needs to be coaligned with the diode laser [39].

We found that using light reflected from one étalon was an excellent method for obtaining a narrowed source for characterizing another étalon. We had a removable beam splitter before the first isolator (see Fig. 4) that was used in conjunction with an additional CFPI [Burleigh 2 GHz free spectral range (FSR) and finesse of 200] to characterize the laser characterization CFPI. This beam splitter was removed in the two-photon absorption experiments. The instrumental response of the 150 MHz FSR measurement CFPI showed slight deviations from the ideal Lorentzian, but the measured width of the response function of 1.6 MHz is very close to the theoretical 1.5 MHz value calculated from the mirror reflectivity.

The measurement CFPI and spectroscopy parts of our experiment were optically isolated with an Optics for Research IO-5-NIR optical isolator (that had about 350-dB isolation) and a tilted neutral-density filter of density unity to reduce the feedback from the measurement CFPI. A Burleigh CFPI 150 MHz free spectral range and a finesse of 100 was used for the measurement étalon. The isolation involved cascading two IO-5-NIR isolators and a quarter wave plate together. This combination produced sufficient isolation to obtain data. The choice of isolation technique and the amount of isolation required are discussed in more detail in Sec. IV B below. We measured the effective isolation by measuring the power reflected back through the isolator. The combined isolation of optics, isolators, and neutral-density filters was on the order of 100 dB or more between the laser and CFPI.

B. Two-photon spectroscopy with semiconductor diode lasers

In this section we describe the theoretical and experimental features of two-photon spectroscopy with semiconductor diode lasers. Its first part deals with the experimental details necessary to obtain a high-quality, two-photon absorption signal, and its second part deals with using atoms as detectors of the second-order statistical properties of the field. Using the Mollow results and the results obtained in Sec. III, we compare the predictions of different laser-noise models with the results of our measurements.

Although our major emphasis is on the measurement of a two-photon transition's linewidth as a function of the laser width, we also describe the difficulties and unique features of performing high-resolution, two-photon spectroscopy with diode lasers. The low power and high sensitivity to optical feedback of diode lasers require precautions that are unnecessary for other laser systems. Doppler-free, two-photon absorption experiments are typically performed with solid-state or dye lasers with a minimum of 50–100 mW of laser power available at the sample. For semiconductor lasers, with only a few mW of available power at the atomic vapor cell, the two-photon signal is reduced by several orders of magnitude because the signal is proportional to the square of the intensity.

There were four requirements for choosing a transition for these experiments: first, the transition has to be at a wavelength accessible to inexpensive diode lasers; second, the transition needs to be strong because of the low laser power; third, the detection wavelength should be far enough away from the excitation wavelength so that simple laser scatter rejection can be used; fourth, the detection scheme should be very efficient. The likely candidate atoms are Rb and Cs because they have two-photon transitions accessible to high-quality off-the-shelf commercial diode lasers. The Rb $5S$-$5D$ transition is an excellent choice, since the intermediate $5P$ states lie almost exactly halfway between the ground state ($5S_{1/2}$) and the excited $5D$ states (see Fig. 5). This resonant enhancement makes this two-photon transition approximately 100 times stronger than a typical strength transition such as a $5S$-$7S$ in Rb, and is essential to help offset the low laser power. The excitation wavelength at 778 nm also lies where excellent $Al_xGa_{1-x}As$ lasers are available. The 420-nm fluorescence wavelength of the $6P$-$5S$ transition has a branching ratio of nearly 40%, is far from the exciting laser's wavelength, and lies in a spectral region where excellent photodetectors are available [40].

Increasing the number density of the gas atoms in the

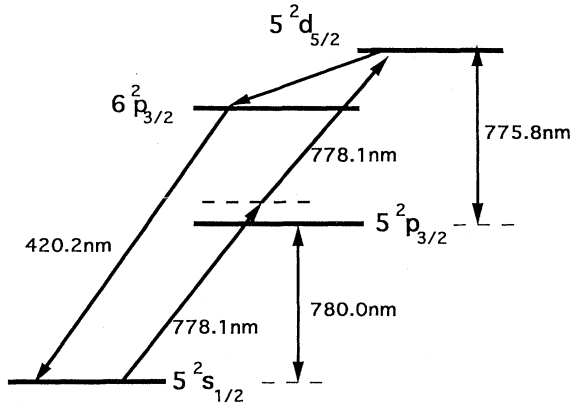

FIG. 5. Gross Rb structure. Note the small energy defect for the intermediate P state in the $5S$-$5D$ transition.

absorption cell should result in a proportional increase in the two-photon signal, but self-absorption and pressure broadening tend to reduce this advantage. Consequently, it is important to determine the optimal number density, which increases by two orders of magnitude for a 100 °C increase above room temperature since self-absorption of the 420-nm fluorescence signal can become significant. We estimated this effect by calculating the temperature dependence of the absorption for a 1-cm path at the center of the Doppler-broadened 420-nm $5S$-$6P$ resonance line. Near 130 °C, where the vapor density is $\sim 10^{13}$ atoms/cm^3, the absorption length for this transition is about 1 cm. These calculations show that at high vapor pressures focusing of the primary laser beams should take place near the cell wall to minimize the absorption path.

In addition to the self-absorption problem, there is also significant self-pressure broadening at higher number densities. Stoicheff and Weinberger measured the self-pressure broadening in Rb to be on the order of a few hundred kHz/mTorr for principal quantum numbers less than 10 [41]. For temperatures near 130 °C, the pressure broadening from Rb itself is less than 1 MHz. In practice, the residual foreign gas in the cell is the dominant source of broadening [41].

Since the rate of two-photon processes is proportional to the square of the intensity, focusing is important in maximizing the signal. Focusing, however, increases the transit-time broadening. In our experiments, the long focal lengths of our lenses combined with our small beams generally result in a beam waist of 40 μm or more. Thus we expect transit-time broadening to be less than a few MHz. Unfortunately, tight focusing of the laser beam requires critical alignment between the counterpropagating beams. This critical alignment also maximizes the coupling efficiency of the retroreflected beam back into the diode laser, and thus increases the optical isolation required.

In our experiment the broadening mechanisms discussed above are the most significant ones, but it is instructive to discuss other residual line-broadening mechanisms. A calculation for the effect of wall collisions [42] shows that for typical cell diameters of a few centimeters the natural linewidth dominates for most transitions.

TABLE I. Sources of line broadening in two-photon spectroscopy of the Rb $5S$-$5D$ transition (modified from [42]).

Type	Origin	Linewidth	Range of values
Doppler broadening	Doppler effect due to thermal molecular motion	$v_0\frac{\nu_0}{c}$ ν_0=center frequency of transition v_0=average speed c=speed of light	~1.2 GHz
Natural broadening	Spontaneous decay of an excited state	$\frac{1}{2\pi\tau}$ τ=natural lifetime	~60 kHz
Lorentz (collision) broadening	Interparticle collisions	$\frac{1}{\pi\tau_{\text{coll}}}$ τ_{coll}=mean time between collisions	<1 MHz
Wall-collision broadening	Particle collisions with the walls of sample cell	$v_0/2\pi L$ v_0=average speed L=cell diameter	<5 kHz
Transit-time broadening	Transit of particles through light beam	$v_0/2\pi a$ v_0=average speed a=beam diameter	<2 MHz

Misalignment of the counterpropagating beams results in a residual Doppler broadening that, however, can be practically eliminated by careful alignment. Additional broadening mechanisms that need to be addressed are power broadening and ac Stark shifts [42], but at our power levels these are negligible. For completeness we have summarized all the above-listed mechanisms together with order-of-magnitude estimates for the Rb $5S$-$5D$ transition in Table I, and show that all the line-broadening mechanisms discussed above are negligible compared to the laser widths used in our experiments.

The light beam was focused into the heated Rb cell, collimated, and reflected back onto itself to produce the counterpropagating beams necessary for Doppler-free two-photon excitation. Part of the beam was sent to the 150-MHz FSR CFPI (see Fig. 4) that served as a frequency marker and laser characterization system. The population excited into the $5D_{5/2}$ state can cascade back to the $5S_{1/2}$ ground state via either the $5P_{1/2}$ or the $5P_{3/2}$ state with a branching ratio of about 3:2 in favor of the $5P_{3/2}$ branch. We chose to detect the fluorescence of the $5P_{3/2}$-to-$5S_{1/2}$ transition at 420.2 nm which is far from that of the incident laser light and is thus straightforward to filter. The $5P_{3/2}$-to-$5S_{1/2}$ fluorescence light was detected with a photomultiplier tube (PMT) (see Fig. 4).

In Fig. 6, we show a typical fluorescence spectrum from two-photon excitation of both the ^{85}Rb and ^{87}Rb isotopes. The hyperfine structure is very well resolved. The two peaks marked C and B correspond to the $6P_{3/2}$-$5S_{1/2}$ $F=2$ and $F=3$ fluorescence signal of the ^{85}Rb isotope, respectively. Peaks D and A correspond to the $6P_{3/2}$-$5S_{1/2}$ $F=1$ and $F=2$ transitions of ^{87}Rb, respectively. The hyperfine splitting of the upper level is not resolved since the laser linewidth is about 15 MHz and the hyperfine splitting is only a few MHz. Evaluation of the data of several scans resulted in a measured hyperfine splitting of the ground state of 3050±5 MHz and 6849±5 MHz for the ^{85}Rb isotope and ^{87}Rb isotope, respectively. These values are within 1% of other measurements [43].

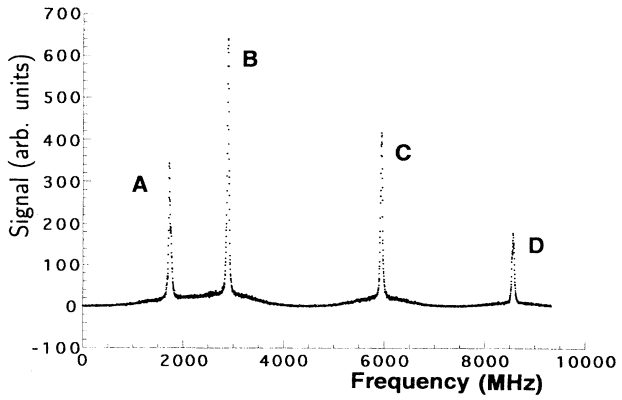

FIG. 6. Two-photon signal showing Rb hyperfine splitting of ground state. Peaks A and D correspond to the $6P_{3/2}$-$5S_{1/2}$ $F=2$ and $F=1$ transitions in ^{87}Rb, respectively and peaks B and C correspond to $6P_{3/2}$-$5S_{1/2}$ $F=3$ and $F=2$ in ^{87}Rb, respectively.

C. Quantum-limited stochastic excitation

Although current tuning of semiconductor lasers is the most common and easiest method for rapid repeatable constant-rate tuning of a laser across an atomic transition, it suffers from possible undesirable effects. The same mechanisms that allow tuning by current also provide avenues for increased bandwidth induced by current noise and pickup from the power supply. Therefore, we have used repeatable, constant-rate temperature tuning to bypass possible problems with technical noise introduced by active power supplies. The result is a quantum-limited laser-noise source with tuning rates exceeding 1 GHz/sec.

The usual difficulties with temperature tuning are nonconstant tuning rates, lack of repeatability, and lack of control of scan length and rate. We have overcome these problems by using a semiempirically derived, digitally generated wave form that drives the Peltier cooler in thermal contact with the aluminum laser mount. We treat the laser mount as a thermal integrator and apply small modifications to the wave form, adjusting for any deviations from ideal behavior. We modified the digitally generated wave form empirically by measuring the frequency tuning rate and adjusting for slight deviations from the ideal rate. The tuning rate was measured with a Burleigh 150-MHz FSR CFPI with finesse of approximately 100. The basic processing involved differentiating the étalon output and locating the peaks of the étalon scans through a zero-crossing technique. The difference in time between the individual peaks was measured and used to determine the rate from the known free spectral range. Figure 7 shows that the tuning rate in our experiments over a period of several seconds is indeed very constant.

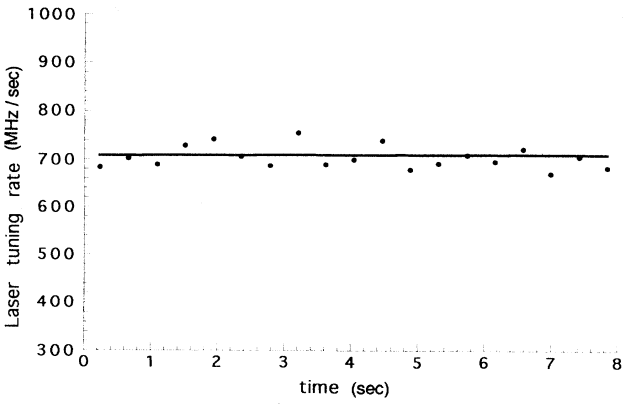

FIG. 7. Measured laser tuning rate over a frequency scan of several seconds. Solid line is a least-squares fit to data.

D. Laser statistics measurements

We measured the two-photon absorption width at four laser powers thus varying the laser width over a range of 7–21 MHz. The two-photon absorption width was found by fitting the Doppler-free component of the ^{85}Rb $F=2$ ground-state transition (see peak C in Fig. 6) to a Lorentzian profile after subtracting the Doppler-broadened component. This transition was chosen since it had the highest signal-to-noise ratio with the simplest Doppler-broadened background of the four detected. The laser width was estimated by fitting the étalon peak closest to the ^{85}Rb $F=2$ ground-state transition to a Lorentzian. Figure 8 shows typical two-photon scans and étalon scans for low (58.0 mA), medium (63.5 mA), and high (79.8 mA) laser currents. The frequency scale in Figs. 8(d), 8(e), and 8(f) was determined by performing direct frequency measurements on the luminescence spectra using an étalon with known free spectral range. Although measurements were made over a factor of 3 in laser power, the intensity of the focused laser in the interaction region was always less than a few hundred mW/cm^2. The atomic density in the Rb cell was 3×10^{13} cm^{-3}. Judging from our signal levels and collection efficiency, we detect 1.5×10^{10} photons/sec. This means that at our intensities each Rb atom cycles only a few times per second. Laser powers of the order of 10^4 times ours would be necessary to saturate the studied transition. This justifies using the second-order perturbation-theory assumption in our modeling.

Both the étalon and two-photon signals are fitted to a Lorentzian. The étalon widths were then corrected for the 1.6-MHz étalon instrumental function. The Doppler-broadened two-photon signal in the background was fitted by a Gaussian and subtracted from the original data leaving only the Doppler-free signal. The Doppler-free signal was then fitted with a Lorentzian. The Lorentzian fits are excellent for both laser and two-photon spectra. Several measurements were made at each power level. The laser width varied less than a few percent during a transition scan of a few seconds, but varied approximately 20% scan to scan. We believe this effect is residual optical feedback changing the laser width slightly from scan to scan.

In Fig. 9, we plotted the signal widths determined this way against the laser widths, and fitted a straight line to the results. The resulting slope is 3.7 ± 0.3, which is in excellent agreement with the theoretical slope of 4 for a phase-diffusion field [5]. The intercept is 10.1 ± 1.0 MHz. This intercept is consistent with residual-gas-pressure broadening in the cell caused by the relatively high operating temperature of the cell. The error bars were estimated by accounting for the statistical as well as possible systematic effects in the fitting procedures. We found the statistical error to be on the order of ±0.1 for the slope. We also found that the subtraction process of the Doppler-broadened background produced an error in the slope of approximately ±0.2. Improvement in this number will probably require better fitting procedures and elimination of the Doppler-broadened background,

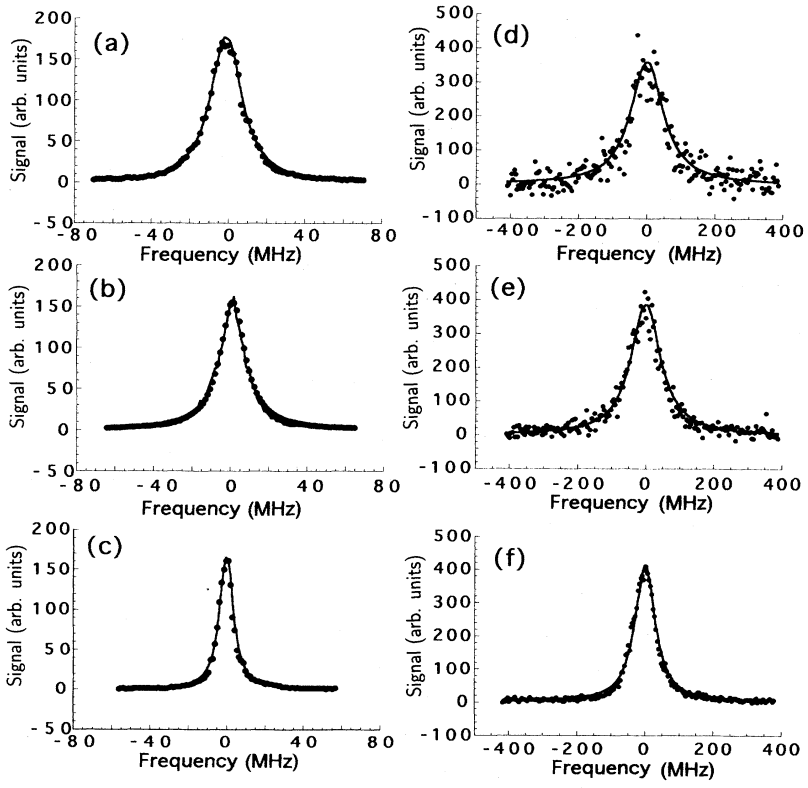

FIG. 8. Etalon scans (left) and corresponding two-photon signals (right) fitted to a Lorentzian. (a),(d) Low power (58.0 mA); (b),(e) medium power (63.5 mA); (c),(f) high power (79.8 mA).

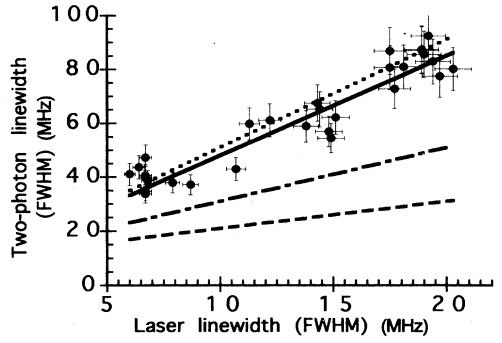

FIG. 9. Two-photon width vs laser width. Solid line: least-squares fit. Dashed lines: Slopes of 1,2, and 4 to guide the eye.

possibly by using the $5S$-$7S$ transition and circular polarization.

V. CONCLUSIONS

Our data corroborate the hypothesis that semiconductor-laser noise is dominated by a pure phase-diffusion process for both first- and second-order statistics. We measured both Lorentzian laser shapes and two-photon absorption shapes. We also measured a slope of nearly 4.0 for the curve which results from plotting the two-photon width vs the laser width. This experimental result combined with our model for amplitude and phase fluctuations provides firm evidence that, in a process sensitive to second-order light fluctuations, the $Al_xGa_{1-x}As$ laser acts essentially as a purely phase-diffusing source of light.

In the process of making these measurements, we have introduced a Doppler-free, two-photon absorption experiment with a semiconductor laser. A method for generating quantum-noise-limited tunable sources based upon temperature tuning the laser is also presented. This technique should be useful for future work involving the study of semiconductor- and fundamental-laser noise in nonlinear atomic processes.

Although our interest in using two-photon absorption has been to study semiconductor-laser noise, such lasers should also be useful for studying a wide range of nonlinear phenomena. It is also clear that Doppler-free two-photon spectroscopy has a wide range of applications. We have shown that diode lasers could serve as compact frequency standards and inexpensive light sources for high-selectivity separation of Rb, radioactive Cs isotopes, and other elements.

ACKNOWLEDGMENTS

Many thanks are due D. S. Elliott for suggestions concerning the modeling of our experiments. L.A.W. and H.J.M. acknowledge financial support by the NSF.

[1] D. S. Elliott, SPIE Proc. **1376**, 22 (1990).
[2] M. Schubert and B. Wilhelmi, *Nonlinear Optics and Quantum Electronics* (Wiley-Interscience, New York, 1986).
[3] Th. Haslwanter, H. Ritsch, J. Cooper, and P. Zoller, Phys. Rev. A **38**, 5652 (1988).
[4] P. Milonni and J. Eberly, *Lasers* (Wiley-Interscience, New York, 1988).
[5] B. R. Mollow, Phys. Rev. **175**, 1555 (1968).
[6] G. S. Agarwal, Phys. Rev. A **1**, 1445 (1970).
[7] F. Diedrich and H. Walther, Phys. Rev. Lett. **58**, 203 (1987).
[8] D. S. Elliott and S. J. Smith, J. Opt. Soc. Am. B **5**, 1927 (1988).
[9] R. Boscaino and R. N. Mantegna, Phys. Rev. A **40**, 5 (1989).
[10] D. S. Elliott, M. W. Hamilton, K. Arnett, and S. J. Smith, Phys. Rev. Lett. **53**, 439 (1984).
[11] D. S. Elliott, M. W. Hamilton, K. Arnett, and S. J. Smith, Phys. Rev. A **32**, 887 (1985).
[12] Y. Kato and B. P. Stoicheff, J. Opt. Soc. Am. **66**, 490 (1976).
[13] A. Mooradian (private communication).
[14] R. E. Ryan, L. A. Westling, and H. J. Metcalf, J. Opt. Soc. Am. B **10**, 1643 (1993).
[15] G. Grynberg and B. Cagnac, Rep. Prog. Phys. **40**, 791 (1977).
[16] S. A. Lee, J. Helmcke, and J. L. Hall, Opt. Lett. **3**, 141 (1978).
[17] C. H. Henry, IEEE J. Quantum Electron. **QE-18**, 259 (1982).
[18] C. H. Henry, IEEE J. Lightwave Technol. **LT-4**, 298 (1986).
[19] M. W. Fleming and A. Mooradian, Appl. Phys. Lett. **38**, 511 (1981).
[20] D. Welford and A. Mooradian, Appl. Phys. Lett. **40**, 865 (1982).
[21] D. Welford and A. Mooradian, Appl. Phys. Lett. **40**, 560 (1982).
[22] J. Harrison and A. Mooradian, Appl. Phys. Lett. **45**, 318 (1984).
[23] M. Sargent, M. O. Scully, and W. E. Lamb, *Laser Physics* (Addison-Wesley, Reading, 1974).
[24] F. T. Arecchi and V. Degiorgio, in *Laser Handbook*, edited by F. T. Arecchi and E. O. Schulz-Dubois (North-Holland, Amsterdam, 1972), Vol. 1, p. 191.
[25] G. H. B. Thompson, *Physics of Semiconductor Laser Devices* (Wiley, Chichester, 1980).
[26] G. P. Agrawal and R. Roy, Phys. Rev. A **37**, 2495 (1988).
[27] C. E. Wieman and L. Hollberg, Rev. Sci. Instrum. **62**, 1 (1991).
[28] J. G. McInerney, SPIE Proc. **1376**, 236 (1990).
[29] D. Lenstra and J. S. Cohen, SPIE Proc. **1376**, 245 (1990).
[30] B. Daino, P. Spano, M. Tamburrini, and S. Piazzolla, IEEE J. Quantum Electron. **QE-19**, 266 (1983).
[31] K. Vahala, C. Harder, and A. Yariv, Appl. Phys. Lett. **42**, 211 (1983).
[32] M. J. O'Mahony and I. D. Henning, Electron. Lett. **19**, 1000 (1983).

[33] K. Kikuchi and T. Okoshi, Electron. Lett. **21**, 1011 (1985).
[34] M. Ohtsu and S. Kotajima, Jpn. J. Appl. Phys. **23**, 760 (1984).
[35] G. Gray and G. P. Agrawal, Phys. Rev. A **37**, 2495 (1988).
[36] R. Loudon, *The Quantum Theory of Light* (Clarendon, Oxford, 1983).
[37] M. Lax, Phys. Rev. **157**, 213 (1967).
[38] J. M. Vaughn, *The Fabry-Pérot Interferometer* (Hilger, Bristol, 1989).
[39] J. Harrison, Ph.D. thesis, MIT, 1987.
[40] C. H. Corlise and W. R. Bogman, Natl. Bur. Stand. (U.S.) Monograph No. 53 (U.S. GPO, Washington, DC, 1962).
[41] B. P. Stoicheff and E. Weinberger, Phys. Rev. Lett. **44**, 733 (1980).
[42] V. S. Letokhov and V. P. Chebotayev, *Nonlinear Laser Spectroscopy* (Springer, Berlin, 1989).
[43] A. Corney, *Atomic and Laser Spectroscopy* (Clarendon, Oxford, 1983).